DESIGN OF MEASUREMENT TECHNIQUES OF ACOUSTIC GLASS SHATTERING SYSTEM

LAU IEK KANG

A project report submitted in partial fulfilment of the requirements for the award of Bachelor of Engineering (Hons.) Electrical and Electronic Engineering

Faculty of Engineering and Science
Universiti Tunku Abdul Rahman

April 2013

DECLARATION

I hereby declare that this project report is based on my original work except for citations and quotations which have been duly acknowledged. I also declare that it has not been previously and concurrently submitted for any other degree or award at UTAR or other institutions.

Signature : _____

Name : LAU IEK KANG

ID No. : 09UEB03656

Date : 10 MAY 2013

APPROVAL FOR SUBMISSION

I certify that this project report entitled **"DESIGN OF MEASUREMENT TECHNIQUES OF ACOUSTIC GLASS SHATTERING SYSTEM"** was prepared by **LAU IEK KANG** has met the required standard for submission in partial fulfilment of the requirements for the award of Bachelor of Engineering (Hons.) Electical and Electronic Engineering at Universiti Tunku Abdul Rahman.

Approved by,

Signature : _____

Supervisor : Mr. See Yuen Chark

Date : _____

Design of Measurement Techniques of Glass Shattering System

ABSTRACT

Objects have the tendency of oscillate at greater amplitude when the frequency of its oscillations matches the system natural frequency. This resonance phenomenon may happen on glasses and cause the glass shattered. Hence, acoustic glass shattering system has been proposed to observe the glass under resonance phenomenon. In this project, a measurement model for acoustic glass shattering system has been implemented. With the implemented measurement model, the natural frequencies of glass could be obtained after the user clicked start button. The program will go through series of sine sweep module automatically and return the measured natural frequencies. Then, user is given option whether to start transmitting acoustic wave at the natural frequency of the glass. The system will start measure the input power of speaker and calculate the time throughout the progress of shattering glass. And finally, the results will be displayed in user interface.

TABLE OF CONTENTS

LIST OF TABLES

LIST OF FIGURES

LIST OF SYMBOLS / ABBREVIATIONS

V_{rms}	root mean square voltage

LIST OF APPENDICES

CHAPTER 1

INTRODUCTION

1.1 Background

Every physical system or object tends to vibrate at particular frequency or a set of frequencies called the natural frequency. Resonance is the phenomenon occurs when the physical system or object is periodically disturbed at one of its natural frequencies. Resonance phenomena occurs with all types of vibration, which is acoustic resonance, nuclear magnetic resonance, electron spin resonance, electromagnetic resonance, resonance of quantum, and mechanical resonance.

Mechanical resonance is a powerful phenomenon which is able to destroy major man-made structures with relatively insignificant forces. The collapse of Tacoma Narrows Bridge is an example of the destructive effect that resonance can have on a physical object. In the last 45 minutes of the life of the Tacoma Narrows Bridge, the oscillation frequency of torsional oscillation caused by aerodynamically induced self-excitation phenomenon(or aerodynamic flutter) is at the natural frequency of the bridge deck, and this ultimately leads to a catastrophic failure(Feldman, 2003). Plenty of similar cases occurred over centuries, such as the collapse of Broughton Suspension Bridge and Angers Bridge(Tilly, 2011), the resonance of Millennium Bridge caused by walking pedestrians(Pavic et al., 2002) etc. These resonance disasters occurred has drawn the attention of scientists and engineers.

The prior art in mechanical resonance is replete with various resonance measuring and testing apparatus such as nondestructive testing apparatus(Taniguchi et al., 2001), stress testing and relieving method and apparatus (Jury, 2000), system for the purpose of stress relieving, fatigue testing and non-destructive load testing(Okubo, 1984), and etc. The ultimate objective of these entire prior art patents is preventing fatigue type destruction and have overlooked the highly destructive force from resonance.

While the body of knowledge on resonance is large, there have been few attempts to use the destructive power of resonance. The mechanical Oscillator from Nikola Tesla has shown the highly destructive power of resonance. In year 1898, Nikola Tesla created “earthquake” from his laboratory using small mechanical variable-frequency oscillator that he attached to a pillar of the building. At that time he recalled the earth trembling “quake” that brought police and ambulances rushing to his Houston Street laboratory(O'Neill et al.).

With the proper controlling, resonance has been proven as a more energy efficiency method to break solid objects. According to (Sellar, 1991), with his laboratory testwork and the scientific laboratory information available, he has made an assumption that the ratio of non-resonant(single blow) to resonant energy to destroy objects is likely to be in the range of 10 to 100. Besides that, Viktor Kozin, a Russian naval engineer has obtained experimental theoretical curves which reveal all the possibilities of breaking ice cover with resonance method in year 2007. According to his research, the power consumption of his design will be several times lower (depending on the thickness of the ice) compared to icebreakers.

1.2 Motivation and Problem Statement

Catastrophic failure of buildings could be caused by relatively insignificant force under resonant phenomenon. Victor Kozin and Sellar have concluded that power consumption of using resonance method to shatter objects can be several times lower

than single blow method, such as explosion. This means unwanted material can be shattered by using an appropriate frequency.

In order to study the behaviour of acoustic resonance, parameters such as natural frequencies and vibration intensity need to be measured. An approach to measure natural frequencies of an object is to knock the target object and then analyze the produced sound. However a relative error within 6% would be expected(Fei et al., 2012). Natural frequencies can be found by generating periodical exciting force to the test object while observing the vibration of the test object, but the measuring process is rather tedious and inefficient. For example, to determine the natural frequencies with AF-ESPI optical system(Lin et al., 2002), function generator has to be adjusted manually throughout the studied range of frequency. Furthermore, operator has to cautiously and gradually tune the function generator if the vibration intensity is increased as the vibrating frequency is in the neighbourhood of natural frequency.

1.3 Project Objectives

The objective of the project "Acoustic Resonance Glass Shattering System" is to observe the behaviour of glasses under acoustic resonance. The project is divided into two sections, which are "Transmitter Design and Calibration of Acoustic Glass Shattering System" and "Design of Measurement Techniques of Acoustic Glass Shattering System".

The objective of this project is to implement a system which includes the measurement of natural frequencies and vibration intensity of a specimen, the measurement of time and power consumed by speaker to shatter the specimen, a sine wave generator module, and a user interface using LabVIEW. The output of sine wave generator will be sent to a signal amplifier before loudspeaker. For more details about the signal amplifier and loudspeaker, please refer to theses "Transmitter Design and Calibration of Acoustic Glass Shattering System" written by Mr. Cheng Xuan Teng.

1.4 Project Scope

Ceramic glasses, wine crystal glasses, and commercial glasses in different shapes will be used to study the behaviour of glasses under acoustic resonance. The behaviour of glasses resonated by 60W acoustic wave will be observed in this project.

CHAPTER 2

LITERATURE REVIEW

2.1 Piezoceramic

The piezoelectronic sound generator shown in Figure 2.1 consists of a built-in oscillating circuit and a simple piezoceramic disk. Piezoceramic disk will vibrate and generate sound when it is driven by the built-in oscillating circuit. Piezoceramic disk is a piezoelectric material. The vibration of the piezoceramic disk can be explained by piezoelectric effect.

Figure 2.1: Piezoelectric Sound Generators (Buzzer)

2.1.1 Piezoelectric Effect

Piezoelectric effect can be described by the phenomena in which the material becomes electrically polarized when subjected to stress and, conversely, become mechanically strained when an electric field is applied(Huang et al., 2005). By taking a piezo disk as example, Figure 2 illustrates the piezoelectric effect.

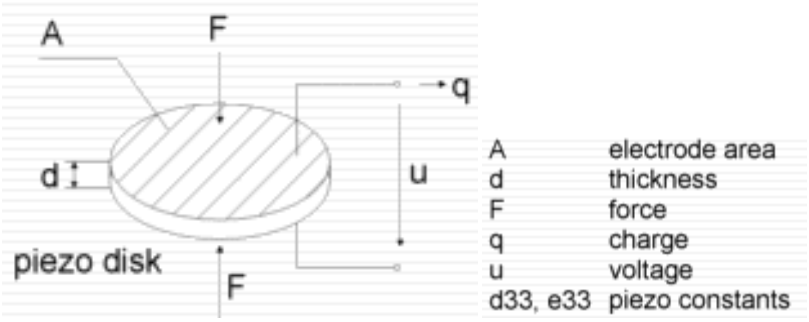

Figure 2.2: Piezoelectric Effect and Its Fundamental Parameters

The piezo disk illustrated in Figure 2 consists of two major parts, which are the piezoceramic material, and seismic mass. One side of piezo disk is seismic mass, where the other side the seismic mass is attached with piezoceramic material.

A force perpendicularly applied to the disk will cause a charge production and voltage difference between two sides. According to Newton's Law, the force applied is equal to the product of seismic mass and acceleration. Direct piezoelectric effect refer to an electric charge *q* is proportional to the applied force.(Tzou and Pandita, 1987) As the seismic mass is constant, the output charge *q* is proportional to the acceleration of the mass. Therefore, piezoelectric materials are often described as active sensors as they produce electrical output only when mechanical stress applied changed.

On the other hand, converse piezoelectric effect will cause piezoelectric material become mechanically strained when an electrical field applied. With the nanodevices made using one-dimensional nanostructures, the deflections of free-standing piezoelectric material (ZnO) are experimentally proved linearly proportional to the voltage applied. The results is shown in Figure 3.(Hu et al., 2009).

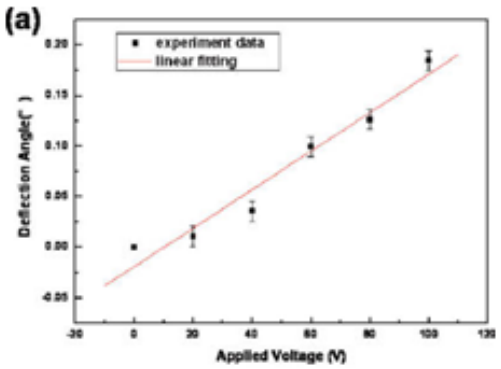

Figure 2.3: Transverse deflection angle of a microbelt as voltage was applied across its width

2.1.2 Piezoelectric Materials Application

Direct piezoelectric effect and converse piezoelectric effect show the ability of using these materials as both sensor and actuator. For example, the force applied on sensor can be measured by identifying the voltage difference across the sensor. Piezoelectric material can be used as vibration sensor, accelerometer, pressure transducers, and damage detector of structures which it is imbedded.

Piezoelectric materials have been widely applied to measure vibration of objects such as vibration of buildings, engine, structures and etc. For example, piezoelectric materials are applied in the development of “intelligent” mechanical system and space structures which emphasize the dynamic measurement and active vibration suppression(Tzou and Tseng, 1990). The direct piezoelectric effect is used to monitors the structural oscillation while the oscillation are suppressed via converse piezoelectric effect. Similarly, the piezoelectric sensors and actuators were integrated to control the vibration of functionally graded material plates(He et al., 2001). The static and dynamic response for functionally graded material plates of aluminium were presented in the article.

2.2 Approaches to Measure Natural Frequencies

A literature search was conducted to investigate the prior art related to the measurement of acoustic natural frequencies. The search was conducted with the keywords “acoustic natural frequency measurement” and resulted in a large number of publications. The keywords “resonant vibration analysis piezoelectric” was then used to reduce the number of search results. “Piezoelectric” was used as keywords in this case because the displacement and velocity of vibration between piezoelectric and the test objects used in this project are similar. Finally, several applicable approaches or technique was found and be categorized into few groups:

2.2.1 Amplitude Fluctuation Electronic Speckle Pattern Interferometry

Electronic speckle pattern interferometry (ESPI), which is also known as TV-holography or electro-optical holography, is an optical measurement technique. It is a full-field, non-contact, real-time measurement method of displacement of deformed bodies(Ma and Huang, 2001). ESPI combines the reference and object beams and directs the beam collinearly toward the detector array of frame-transfer charge-coupled device (CCD), which interfaces with computer for video processing of spackle patterns. The resultant fringe patterns of ESPI are displayed on television-monitor in real-time (about 30ms). An example schematic diagram of ESPI setup for out-of-plane vibration measurement is shown in Figure 2.4.(Lin et al., 2002)

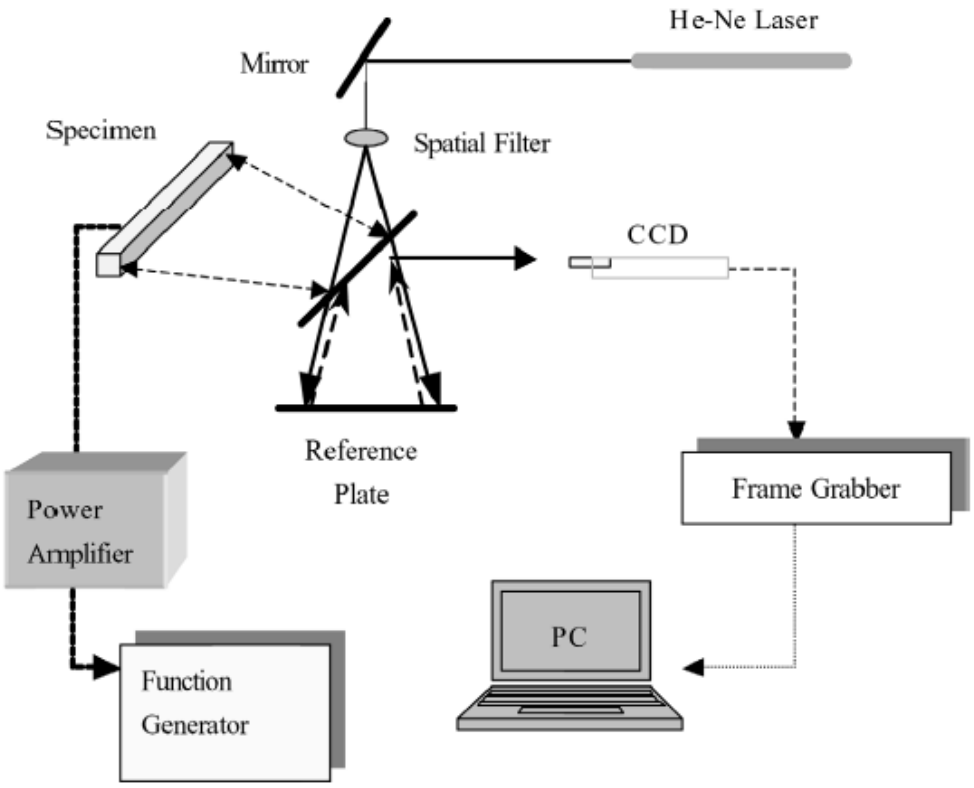

Figure 2.4: Schematic Diagram of ESPI Setup for Out-of-plane Measurement

Due to the real-time nature of EPSI and more insensitive to environment than holography, it has become a widely used technique in academic researches and engineering applications like vibration measurement. The first publication on ESPI is by Butters and Leendertz who investigated the out-of-plane displacement of a vibrating disk (Butters and Leendertz, 1971). Since then, the technique of ESPI was applied area of deformation analysis, especially vibration measurement. However, without additional image or signal processing procedures, the fringe pattern obtained directly by ESPI is rather difficult to observe.

In order to improve the contrast of fringe patterns, Huang and Ma (Huang and Ma, 1998), (Ma and Huang, 2001) further developed the amplitude-fluctuation ESPI (AF-ESPI) based on the effort of Wang *et al* (Wang et al., 1996). Based on the results from the publications of Huang and Ma, AF-ESPI displayed the interferometric fringe patterns has higher quality for the identification of natural frequencies and mode shapes.

AF-ESPI was used for various vibration analyses. Lin *et al* analyzed the vibration of piezoelectric materials by optical methods (Lin et al., 2002). AF-ESPI was used in their work to study the natural frequencies and mode shape of vibrating piezoelectric materials. The results were validated by experimental results from laser Doppler vibrometer and also the theoretical results by means of Galerkin method and finite element method.

Lin and Ma used AF-ESPI in their work to analyzed the characteristics of piezoelectric disks with partial electrode designs(Lin and Ma, 2004). A good agreement between the experimental result from AF-ESPI and laser Doppler vibrometer can be seen from the results. Huang *et al* used AF-ESPI to investigate the resonant vibrations of piezoceramic annular disks(Huang et al., 2005). The publication concluded that AF-ESPI method has advantages of non-contact, real-time, and high-resolution measurement for studying the vibration of piezoceramic annular disks.

2.2.2 Laser Doppler Vibrometer

Laser Doppler Vibrometer(LDV) is an optical measurement technique which uses optical interferometry to measure pointwise displacement(Lin and Ma, 2004). Based on the Doppler Effect, the frequency of the laser beam will be shifted if the surface orthogonal to the laser vibrates(Bloss and Rao, 2002). The primary advantage of using LDV is the non-contact nature of the vibrometer. The non-contact nature would eliminate mass loading of the specimen and therefore a more accurate results would be obtained.

Lin *et al*(Lin et al., 2002) used laser Doppler vibrometer system to find the natural frequencies of piezoelectric material. An amplified swept-sine excitation signal was input to the piezoelectric specimen while the laser beam was directed to a specific point of the upper surface of the specimen. Finally the measured data in time domain was converted into frequency domain and the natural frequencies was identified from the spectrum response curve. The good correspondence of the

experimental data from LDV system and theoretical results by means of the Galerkin method and FEM demonstrates the LDV system proposed is applicable in vibration analysis for piezoelectric materials. Figure 2.5 illustrates the schematic diagram of LDV measurement system used in this publication.

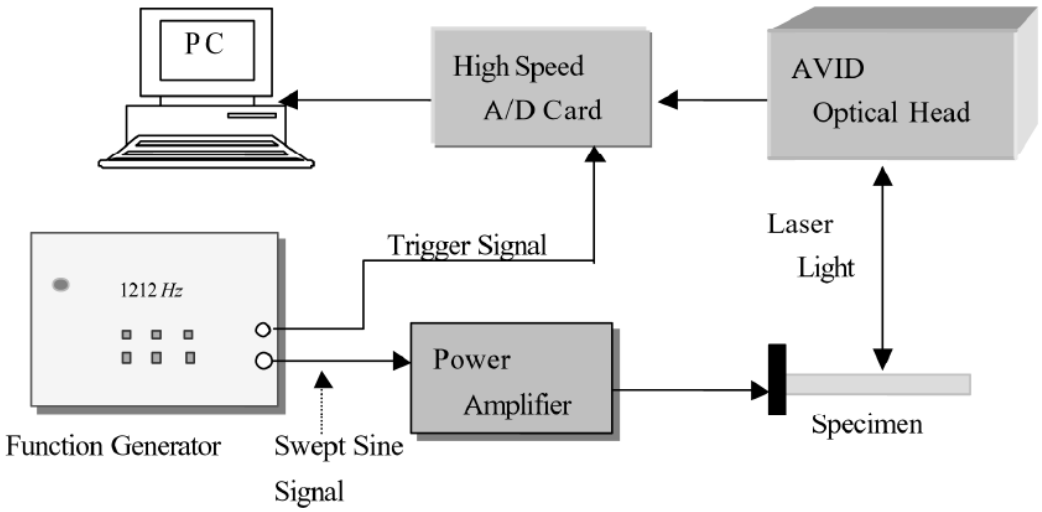

Figure 2.5: Schematic diagram of LDV Measurement System for Natural Frequencies Extraction

Lin and Ma used AF-ESPI, LDV and impedance analysis to investigate the resonant characteristics of piezoelectric disks with full and partial electrode designs (Lin and Ma, 2004). LDV system was used to obtain the resonant frequencies of the transverse vibration. Transverse resonant frequencies obtained from AF-ESPI methods were used to compare with the results measured by LDV system. The difference of frequencies measured by LDV and AF-ESPI is less than 3%.

Huang *et al* carried a theorectical, numerical, and experimental investigation on resonant vibrations of piezoceramic annular disks (Huang et al., 2005). Experimental measurements obtained by AF-ESPI, LDV, electrical impedance were used to compare with the numerical results calculated with finite-element calculations and theoretical analysis. LDV system was used to measure the resonant frequencies of transverse vibrations. The results show that the first six transverse resonant frequencies of piezoceramic annular disks obtained by the AF-ESPI and LDV are in excellent agreement with the differences below 0.6%.

2.2.3 Acoustic Method

Chang-hui suggested the method of measuring natural frequencies based on the knocking method(Chang-hui, 2005). Knocking method is a typical transient excitation method used to measure natural frequencies. In fact the sound frequencies generated by knocking an object are natural frequencies of the object. Fei *et al* measured the natural frequencies for the components of train wheel-bearing based on acoustic method(Fei et al., 2012). A microphone was used in their designs to convert the sound pressure to electrical signal. The electrical signal was acquired by a data acquisition card for dynamic signal from NI Company. After filtering, interception, windowing the acquired data, the natural frequencies was observed from the frequency response spectrum. Example of the obtained results from his publication is shown in Figure 2.6 and Figure 2.7.

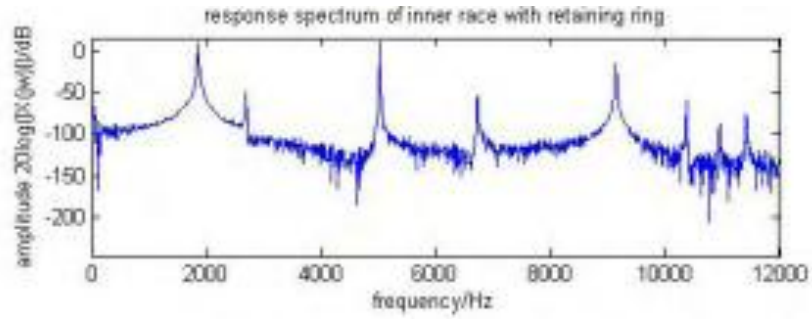

Figure 2.6: Frequency Response Spectrum of Inner Race with Retaining Ring

Type of vibration		Order 2	Order 3	Order 4
flexural vibrations (Hz)	ANSYS	1887	0.27	7.813
	measurement	1855	0.27	7.813
	relative error	1.70%	0.27	7.813
Torque Vibration (Hz)	ANSYS	2741	0.27	/
	measurement	2695	6871	/
	relative error	1.68%	1.94%	/
Sliding vibration (Hz)	ANSYS	10517	/	/
	measurement	10380	/	/
	relative error	1.30%	/	/

Figure 2.7: Comparison of Theoretical and Measured Results for Inter Race (with Retaining Ring)

In contrast to optical methods, the procedures of acoustic method are simpler and more convenient. However, a relative error within 6% would be expected when compared the simulated frequencies and measured frequencies.

2.3 Conclusion

Results have shown that the two optical methods have the advantages of noncontact, real-time, and high-resolution measurement for vibration analysis. However the experiment setup is complicated and the instruments for optical methods are expensive (more than RM20,000) and not easy to be found from teaching laboratory. Piezoceramic has overcome these issues and had been chosen as the vibration sensor for this project. Another important property of piezoelectric transducer is their speed of response, which allows them to register a fast process like parameters of explosion(Kerbel and Artjuhina, 2000). Finally, a procedure was derived from the techniques of acoustic method(Fei et al., 2012) and acoustic emission testing(Beattie, 1983). The details of the procedure will be discussed in next chapter.

CHAPTER 3

METHODOLOGY

3.1 Overview of Acoustic Glass Shattering System

A block diagram of acoustic glass shattering system is shown in Figure 3.1. A personal computer will be used to communicate with NI sbRIO-9632XT. NI sbRIO-9632XT is an embedded control and acquisition device which integrates a real time processor, a user-reconfigurable field-programmable gate array (FPGA), and I/O. In this system, NI sbRIO-9632XT will send signal to power amplifier and speaker to generate sound. Vibration sensor will be used to convert the vibration strength of sample to electrical signal. By doing this, the response of sample to the generated sound could be observed.

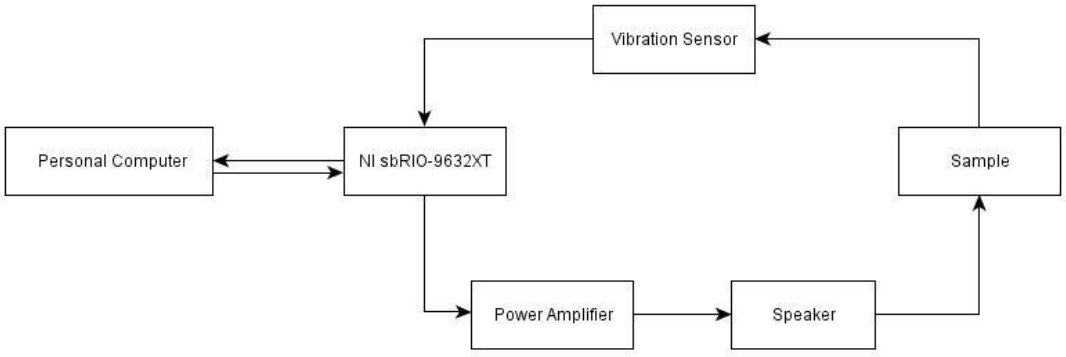

Figure 3.1: Block Diagram of Acoustic Glass Shattering System

Figure 3.2 describes how the overall process of acoustic glass shattering system runs. Details for the implementation of each of the blocks will be discussed in next section.

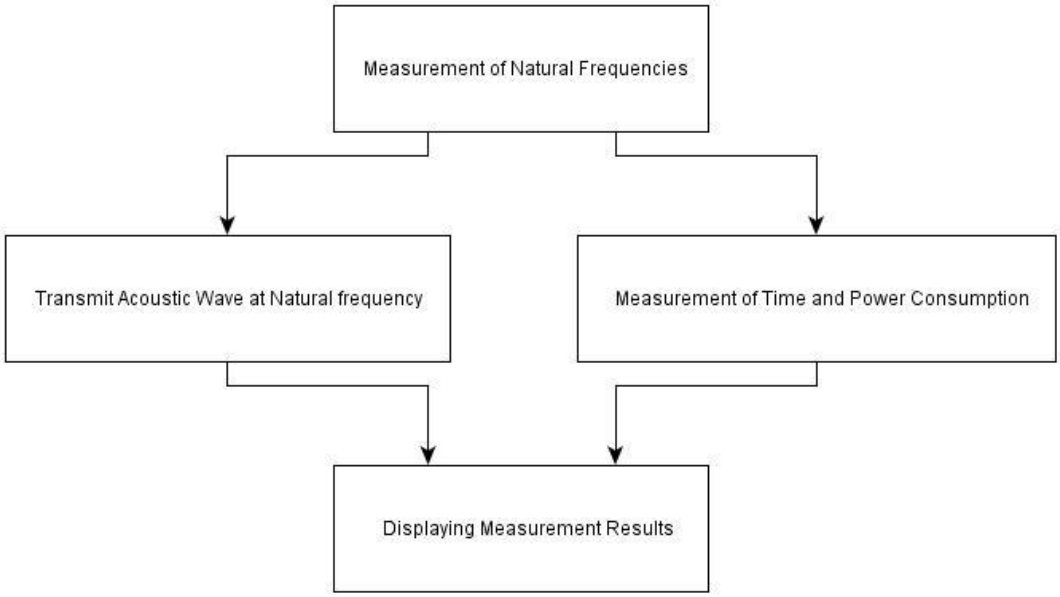

Figure 3.2: Overall Flow Chart of Acoustic Glass Shattering System

3.2 Details of the Overall Flow Chart

The implementation of each of the block shown in Figure 3.2 is discussed in this section. The programming tool used to implement this project would be LabVIEW, which is a graphical programming environment developed by National Instrument.

3.2.1 Measurement of Natural Frequencies

Sine sweep method is adopted in this project to measure the natural frequencies of an object. Sine sweep method involves sweeps of sine vibration across a frequency range and measurement of vibration strength of sample at each of the frequency. By doing this, the natural frequencies could be obtained from the frequency spectrum.

Each of the peaks observed from the frequency response spectrum represents a natural frequency.

Hardware needed to measure natural frequencies includes a personal computer, NI sbRIO-9632XT, power amplifier, speaker, and piezoceramic (vibration sensor). The program needed for the implementation includes a module to generate sine wave, a module to implement sine sweep signal using sine wave module, a module to calculate root mean square value of input signal, algorithm to filter noise and detect local maxima, and a user interface. Verifications will be made during the developing phase to ensure that every module is function properly.

Instead of measuring the vibration strength at every Hz within the frequency range of 150 Hz to 5000 Hz, the program will measure the vibration strength every 25 Hz. Estimation of natural frequencies can be done by locating all local maxima after filtering noise. Noise filtering is achieved by calculating the means and standard deviation of all the measured vibration strength. Whichever vibration strength less than the sum of means and standard deviation are considered noise. Figure 3.3 illustrates the program flow for this process. Blocks in orange colour indicate the program runs in FPGA, while blocks in grey colour indicate the program runs in personal computer.

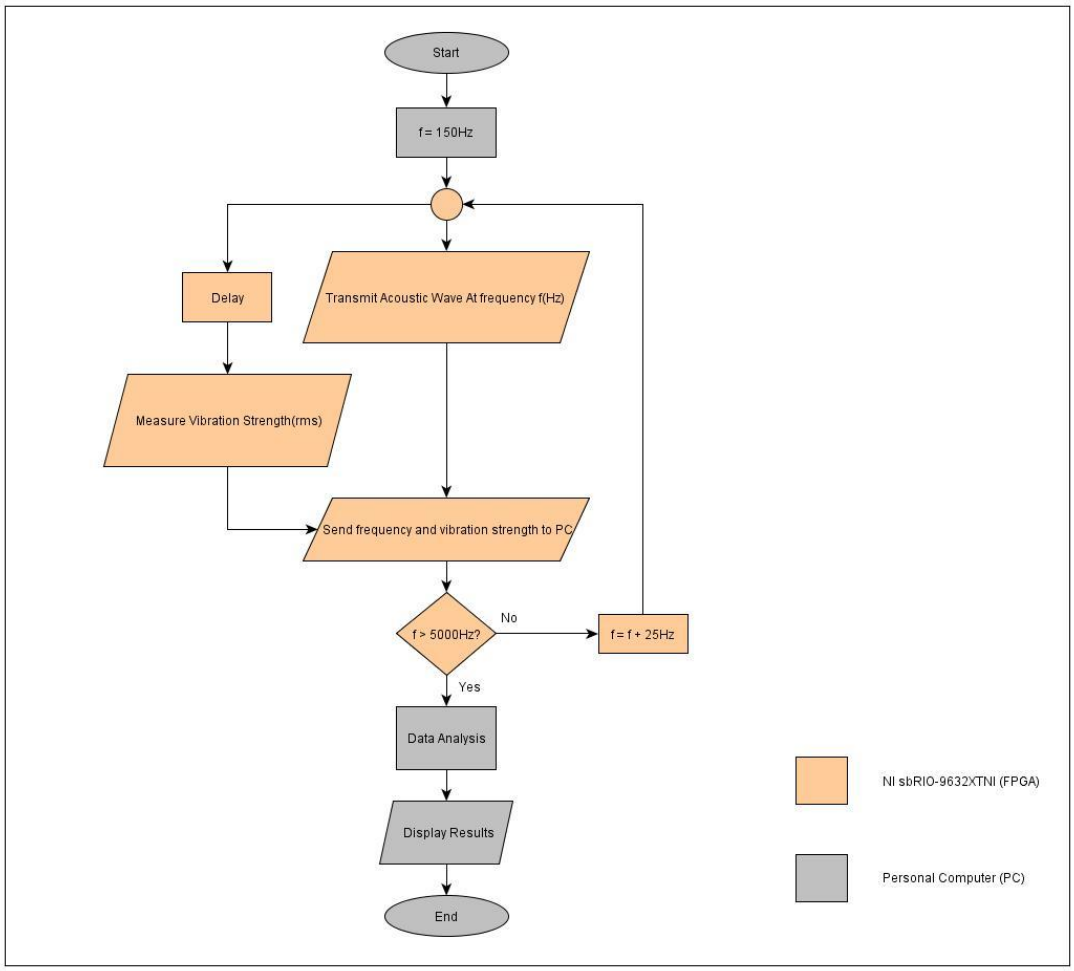

Figure 3.3: Estimation of Natural Frequencies

Sine sweep signal similar to Figure 3.3 will be transmitted for each local maxima, where

Initial frequency = local maxima – 25Hz
Final frequency = local maxima + 25Hz
Step size = 1Hz

Natural frequency can be found from these 50 measured vibration amplitude. The frequency with the highest vibration amplitude is the natural frequency of the sample.

Compared to the method (says method A) which measures the vibration strength Hz by Hz to find the natural frequencies, this estimation method (says method B) can significantly reduce the time for the measurement. The calculation of time saved using this estimation method is shown:

$$t_A = (f_2 - f_1) \times t_0$$

$$t_B = \left[(2 \times N \times \Delta f) + \frac{\Delta f}{f_2 - f_1}\right] \times t_0$$

$$\%time\ reduced = 1 - \frac{t_B}{t_A}$$

$$= 1 - \frac{\left[(2 \times N \times \Delta f) + \frac{\Delta f}{f_2 - f_1}\right]}{(f_2 - f_1)}$$

$$= 1 - \frac{\Delta f + (2 \times N \times \Delta f) \times (f_2 - f_1)}{(f_2 - f_1)^2} \quad (3.1)$$

Where

N = number of natural frequencies of sample

t_0= time required for each cycle

t_A = time consumed using method A

t_B = time consumed using method B

f_1= initial frequency

f_2= final frequency

Δf= frequency step size

The flow chart shown in Figure 3.3 illustrates the estimation method with initial frequency of 150Hz, final frequency of 5000Hz, and frequency step size of 25Hz. If three natural frequencies were detected using the method shown in figure 3.3, by using the derived equation (3.1), 96.91% of time would be saved using method B.

3.2.2 Measurement of Time and Power Consumption

Measurement of time and power consumption will be made when speaker is transmitting acoustic wave towards sample. These quantitative data will be meaningful when the sample is shattered by speaker, as the quantitative data describe "how much energy does speaker consumed to shatter the sample" and "how long does the process of shattering take".

The measurement of time can be done by using the "Tick Count Express VI" which can be found in LabVIEW-FPGA. The VI, shown in figure 3.4, can be configured to return an unsigned 32-bits integer which represents the time in milliseconds.

Figure 3.4: Tick Count Express VI

The measurement of power consumption of speaker can be implemented by measuring the input voltage of the speaker. A root mean square function will be implemented to calculate the V_{rms} of the input signal. The measurement will be done by using 16-bits ADC which can be found from NI sbRIO-9632XT. However the nominal input range of the analogue input is ±10V while the input signal could be up to ±30V or even more. A voltage divider circuit with the scaling factor of 10% will be implemented to overcome this issue.

3.2.3 Transmit Acoustic Wave at Natural Frequency

The natural frequency with the highest vibration amplitude will be chose from the list of detected natural frequencies. A sine wave will be sent at the natural frequency by using the implemented sine wave generator module. The vibration of the sample will

be measured simultaneously and continually. The measured vibration indicates the status of the sample. A sudden impact measured indicates the shattering of the sample, while very weak vibration shows that the sample is already shattered or cracked. If the vibration strength of sample under resonant frequency is X, vibration strength larger than 1.5X will be defined as sudden impact, while vibration strength less than 0.5X is defined as 0.5X. If a suddenly impact or weak vibration measured, program will stop transmitting and enter the last step, which is to display the results. Or the program will terminate after the system transmits acoustic wave for 30 seconds.

3.2.4 Displaying Measurement Results

The calculated time and measured power consumption will be displayed in this section. Along with the frequency spectrum from 100Hz to 5000Hz, a Boolean indicator to indicate whether the sample is shattered, and the list of measured natural frequencies in integer, the user interface is formed.

3.3 Behaviour of Glasses under Acoustic Resonance

Upon the completion of project "Transmitter Design and Calibration of Acoustic Glass Shattering System" (covered by Mr. Cheng Xuan Teng), optimum distance between transmitter and glasses and a suitable acoustic transmitter (loudspeaker) will be chosen to study behaviour of glasses under acoustic resonance. Different material and shapes of glasses will be used as samples. The natural frequencies of glasses will be measured using the measurement described under the section3.2.1. Then, system will start transmitting 60W acoustic wave at the natural frequency of specimen and determine whether the sample can be shattered.

CHAPTER 4

RESULTS AND DISCUSSION

4.1 Software Architecture

The main program VI in host computer linked all modules to achieve the project objectives. The software flow chart of the main.VI is shown in Figure 4.1.

Main.VI sent instruction to FPGA_Swept_sine.VI after operator clicked start button. System started to generate sweep sine vibration while measuring the vibration strength. Measurement was plotted in a vibration strength verses frequency XY graph in real time. Data analysis was performed to locate peaks of the XY graph. Sine sweep was then performed for each of the peak to find out the exact natural frequencies. The natural frequency with the strongest vibration was chosen and displayed to operator. The program would not continue the process until the operator clicked "GO!" button. Operator was given chances to cover their ears and kept distance from the sample before click the "GO!" button. After the button clicked, loudspeaker transmitted acoustic wave at 60W. The program stopped when the sample shattered or the process run for 30 seconds. Finally, results was displayed which include time taken for the process, output power of speaker and the total energy consumed by the speaker.

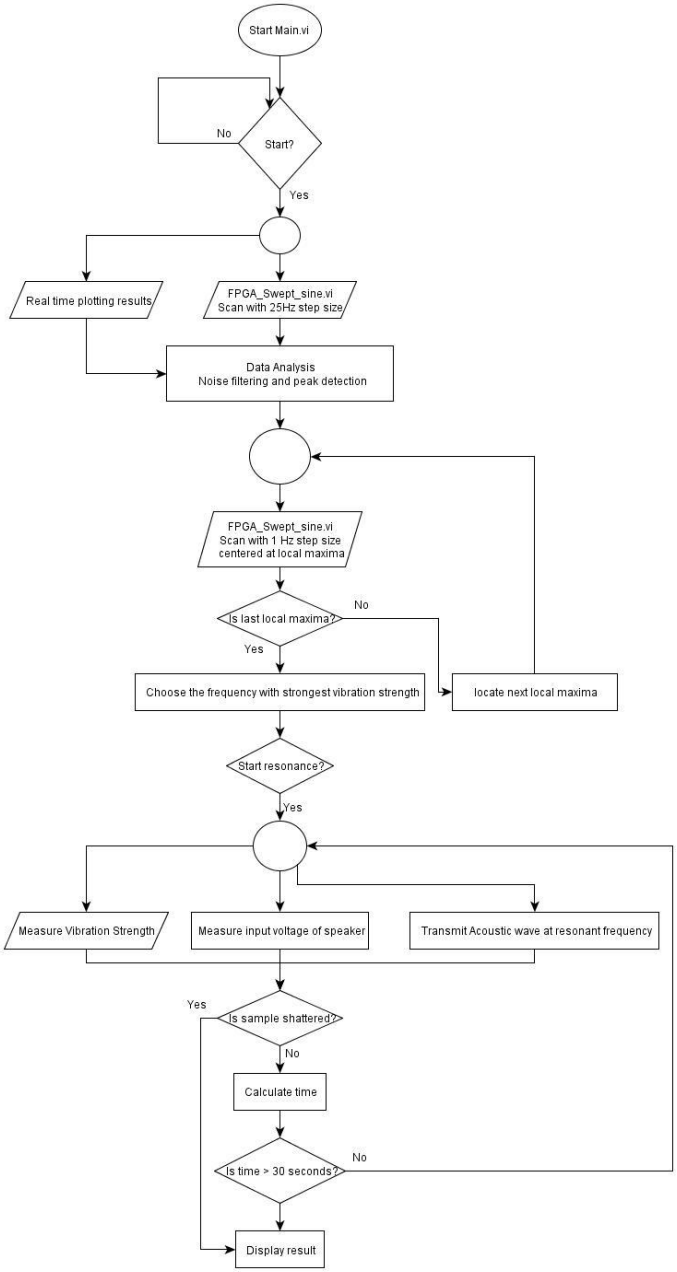

Figure 4.1: Flow chart of main program

4.2 Implementation and Results Verification of Modules

Several modules were implemented to aid Main.VI in performing the tasks shown in Figure 4.1. The implementation of each module is shown in this section, along with the verification of the results.

4.2.1 Implementation and Results Verification of Sine Wave Generator

A sine wave generator module was implemented using the DAC from sbRIO-9632XT board. The DAC from sbRIO board has the resolution of 16-bits and the highest rate of 100kS/s. This sine wave generator was implemented by updating the DAC output voltage every 10 microsecond. To verify the module, setting of frequency at 1000Hz, and amplitude at 5 was inserted. Then, the output of the DAC was captured using TDS 1012B digital storage oscilloscope and is shown in Figure 4.2.

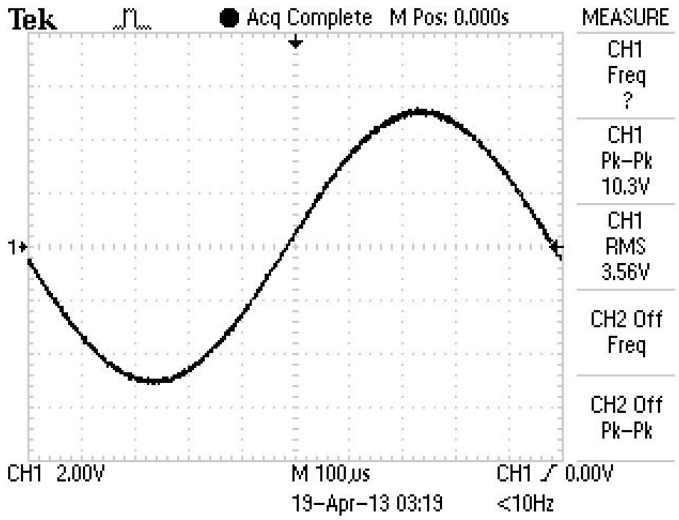

Figure 4.2: Output of Sine Wave Generator Module

4.2.2 Implementation and Results Verification of RMS Meter

A module to calculate root mean square of continuously varying signal was implemented using ADC of sbRIO-9632XT. First, a user defined variable “Delay” will instruct the module to idle for certain time. Then the ADC starts collecting data for 20ms at the sampling rate of 150kS/s. A conditional flag “output valid” will rise after the module calculated the root mean square of 3000 samples.

The results were verified using DG1022 function generator from company RIGOL and TDS 1012B digital storage oscilloscope. The signal from function generator was fed to oscilloscope and ADC in parallel. The value returned from module match the RMS measured from oscilloscope within the range of 150Hz to 5000Hz.

The RMS module serves for two purposes, which is to measure the vibration strength from piezoceramic (vibration sensor) and the input voltage of speaker. The nominal input range of ADC is ±10V, while the highest output voltage from the power amplifier is 50V. Therefore a voltage divider circuit was built to measure the input V_{rms} of speaker and is shown in Figure 4.3.

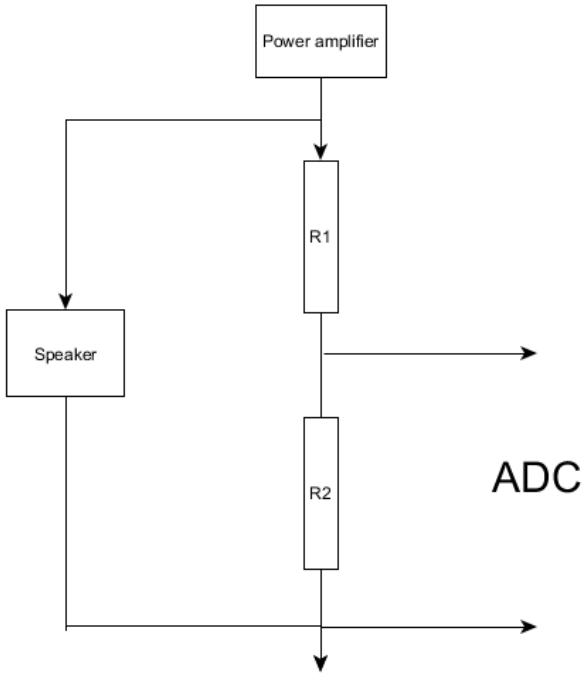

Figure 4.3: Voltage Divider for Measurement of Speaker Power

The measured resistance of R1 and R2 is 9820 Ω and 984Ω respectively, and the measured resistance of speaker is 12.0 Ω. With the known voltage divider ratio, resistance of speaker, and the input V_{rms} of speaker, the input power of speaker can be calculated.

4.2.3 Implementation and Results Verification of Swept Sine Module

Swept sine module was implemented in such a way that it will scan a range of frequency while measuring the vibration strength with RMS meter module. Meanwhile, the frequency and measured vibration strength will be sent to host computer for displaying and data analysis. In this system, swept sine module acts as the main program in sbRIO-9632XT and it ensure the synchronization among modules and the sequence of steps and modules.

Upon the implementation of this module, natural frequencies can be measured by the system. Figure 4.4 shows the plotted X-Y graph based on the results returned from this module. The natural frequencies of 874Hz and 1441Hz were detected and displayed below the X-Y graph. The vibration of sample was strong enough to be observed using naked eyes when it was under periodical disturbance at resonant frequency. Therefore the measured frequencies with this module are the natural frequencies of the sample.

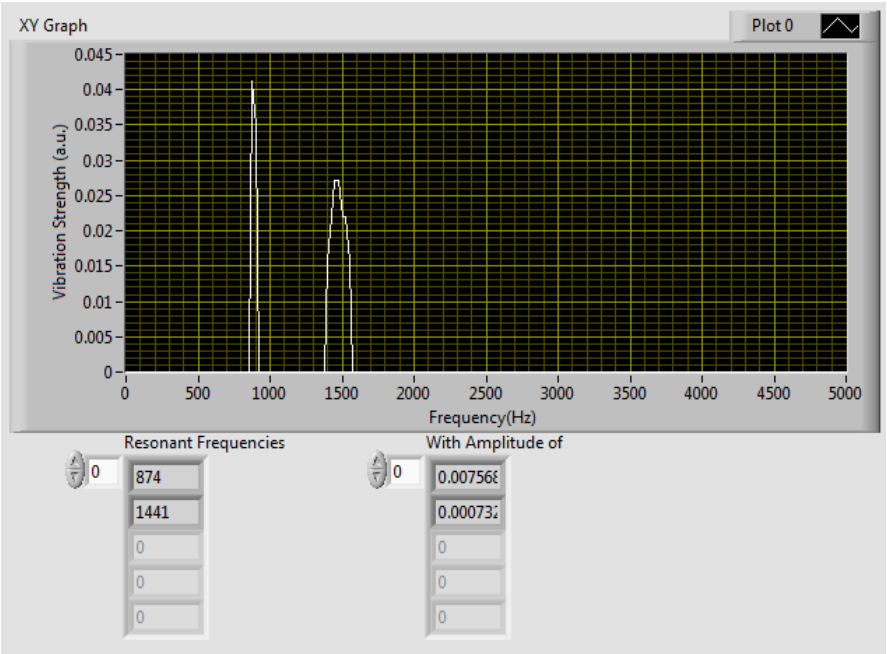

Figure 4.4: Frequency Spectrum and Measured Resonant Frequencies

4.3 Measurement of Natural Frequencies

Sine sweep method was adopted in this project to measure the natural frequencies of an object. Sine sweep method involves sweeps of sine vibration across a frequency range and measurement of vibration strength of sample at each of the frequency. Figure 4.5 shows an example of frequency response function of a glass from the frequency range of 150Hz to 3000Hz. After noise filtering, six peaks were detected by system. Then, swept sine vibration was applied for each peak. For example, first peak was detected at 450Hz. A swept sine from 425Hz to 475Hz was launched to determine the exact natural frequency. Figure 4.6 shows the results of swept sine for first peak, where the X-axis was scaled to 439Hz to 458Hz.

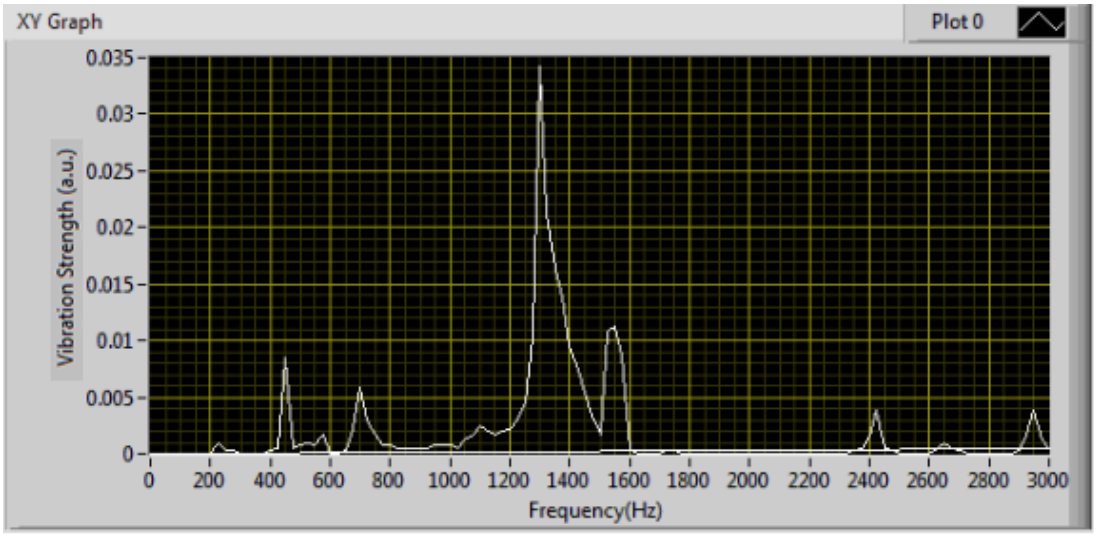

Figure 4.5: Frequency Response Functions of Glass from 150Hz to 3000Hz

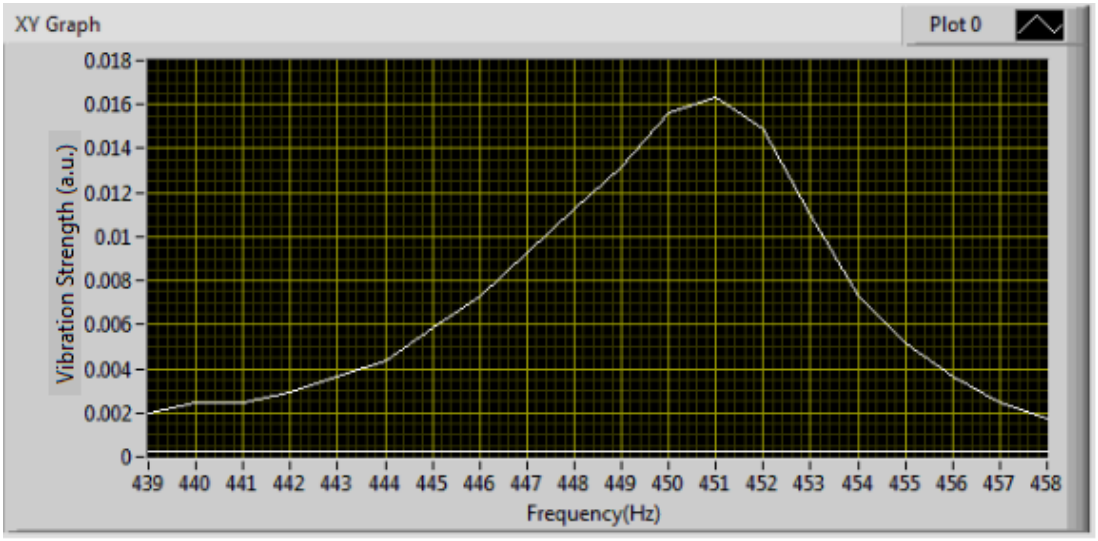

Figure 4.6: Frequency Response Functions of Glass from 439Hz to 458Hz

While developing the measurement model for natural frequencies, piezoceramics in different size were used as vibration sensors. After running the swept sine module, different natural frequencies were obtained from same glass. This is because the measurement of the dynamic behaviour of a structure in terms of Frequency Response Functions (FRFs) is always vulnerable to measurement errors. The mass-loading effect of transducers is one of the sources of error in modal testing.(Ashory, 2002) The piezoceramic mounted on the specimen changes the dynamics of the structure and introduces errors into the measured FRFs.

From a practical point of view, comparison between natural frequencies of the measured frequency response functions is a suitable way of assessing the quality of the measurement. Therefore a series of tests had been run through. Two piezoceramics in different size were used as vibration sensor and run through tests individually. The two piezoceramics, which are piezoceramic A, and B, with the diameter of piezoelectric material of 1 inch and 0.3 inch respectively, is shown in Figure 4.7. Each piezoceramic was used as vibration sensor and attached at different place of sample. Vibration sensors were mounted to samples using Shimato isolation tap. The experiment setups are shown in Figure 4.8, Figure 4.9, and Figure 4.10, where the piezoceramic was attached at opposite face, side face and in front of the loudspeaker.

Figure 4.7: Piezoceramic A, and Piezoceramic B

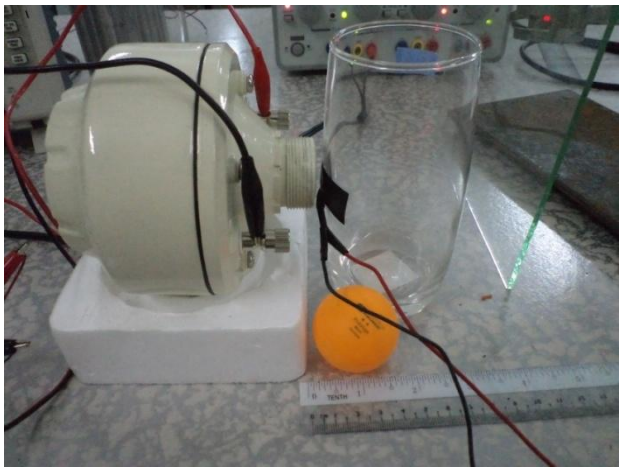

Figure 4.8: PIezoceramic Attached in Front of Loudspeaker

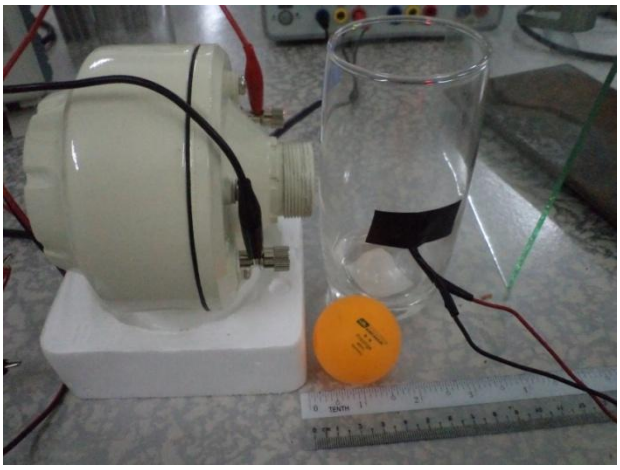

Figure 4.9: PIezoceramic Attached at Side Face of Loudspeaker

Figure 4.10: PIezoceramic Attached at Opposite Side of Loudspeaker

Three glasses, glass X, glass Y, and glass Z shown in Figure 4.11 had been used as samples for the tests.

Figure 4.11: Glass X, Glass Y, and Glass Z

In summary, two vibration sensors were used to measure three different glasses at three different attached places. Measurement had run for three times for each combination (for example piezoceramic A, attached at front side of glass X) and a relative difference within 0.8% was observed. This relative difference was acceptable and therefore it will not be included in tables.

The results of every combination mentioned were shown in Table 4.1 and Table 4.2. The Peak (units) shown in Table 4.1 and Table 4.2 represents the local maxima detected from waveform, and the order of frequency 1^{st}, 2^{nd}, 3^{rd} was

arranged according to the vibration strength at that particular frequency. The highlighted data represent the natural frequency of sample.

Table 4.1: Results of Natural Frequencies Obtained Using Sensor A and Sensor B (Range = 1cm, Input Power of Speaker = 65mW)

	Sensor A (1")			Sensor B (0.3")		
	Front	Side	Opposite	Front	Side	Opposite
Glass X						
Peak(units)	10	3	5	1	1	1
1st (Hz)	2000	1383	1385	1395	1400	1399
2nd (Hz)	1347	1875	3346	-	-	-
3rd (Hz)	900	3348	900	-	-	-
Glass Y						
Peak(unit)	10	3	2	0	0	0
1st (Hz)	878	878	875	-	-	-
2nd (Hz)	1773	2120	1444	-	-	-
3rd (Hz)	4010	4020	-	-	-	-
Glass Z						
Peak(unit)	2	1	1	0	0	0
1st (Hz)	2695	2695	2698	-	-	-
2nd (Hz)	1587	-	-	-	-	-
3rd (Hz)	-	-	-	-	-	-

Table 4.2: Results of Natural Frequencies Obtained Using Sensor A and Sensor B (Range = 1cm, Input Power of Speaker = 1.04W)

	Sensor A (1")			Sensor B (0.3")		
	Front	Side	Opposite	Front	Side	Opposite
Glass X						
Peak(unit)	12	7	3	1	1	1
1st (Hz)	1376	1378	1378	1400	1399	1397
2nd (Hz)	3336	3348	3334	-	-	-
3rd (Hz)	3525	3725	3725	-	-	-
Glass Y						
Peak(unit)	9	15	13	9	2	2
1st (Hz)	874	874	874	3836	880	882
2nd (Hz)	3669	2138	2120	882	4034	4000
3rd (Hz)	1659	175	4033	3950	-	-
Glass Z						
Peak(unit)	11	11	19	0	0	0
1st (Hz)	2694	2695	2825	-	-	-
2nd (Hz)	826	175	2674	-	-	-
3rd (Hz)	175	653	819	-	-	-

Table 4.1 shows the results measured with 64mW (input power of speaker). Then, the input power of speaker was increased to 1.04W, run through the tests again and the measurement was written in Table 4.2. By comparing the results in Table 4.1 and Table 4.2, piezoceramic A (with bigger piezoelectric material mass) has higher sensitivity compared to piezoceramic B. Natural frequencies of glass X, glass Y, and glass Z can be measured using piezoceramic A when the speaker was supplied with 64mW only. However for the case "piezoceramic A attached at the front of glass X" and "piezoceramic A attached at the opposite of glass X", incorrect frequency was detected. The 1st natural frequency is believed to be the natural frequency of piezoceramic itself or the resonant frequency of speaker.

The obtained natural frequency using piezoceramic A is lower than piezoceramic B. The reason of this trend is caused by the mass loading effect. Mass loading effect is the effect caused by adding additional mass to a dynamic structure. By adding an additional mass, the dynamic behaviour of the structure will be changed. Piezoceramic A with higher mass would reduce the natural frequency of structure more; structure refers to the combination of piezoceramic and the sample. Therefore the measured natural frequencies using piezoceramic A is slightly lower than piezoceramic B. From the table 4.1 and table 4.2, resonance effect in glass X is the strongest while the vibration of glass Z is the weakest under the resonance. In other words, glass X can be shattered with least acoustic power.

Clearly, the vibration sensor with bigger size has higher sensitivity. However, sensor with bigger mass has more mass-loading effect on the test structure. Among the available piezoceramics, the one which can measure the responses of the glass in the desired frequency range and has least mass loading effect is the best choice. Furthermore, the attachment of the vibration sensor should neither facing the speaker nor at the opposite of the speaker.

CHAPTER 5

CONCLUSION AND RECOMMENDATIONS

5.1 Conclusions

As a conclusion, the objectives of this project are partially achieved. A measurement model for the acoustic glass shattering system has been implemented. The measurement model includes the measurement of natural frequencies and vibration intensity of specimen, the measurement of time and power consumed by speaker if success to shatter the specimen, a sine wave generator module, and a user interface using LabVIEW. To achieve these, several modules have been implemented and linked together. The functionality of every module has been verified to ensure the overall performance of the system. The natural frequencies of specimen have been measured using the implemented system.

The behaviour of glasses under acoustic resonance has been observed. Under resonance, glasses are vibrating. However, most of the glasses could not be shattered due to the power limitation of the system. Among ceramic glasses, wine crystal glasses, and commercial glasses in different shapes, wine crystal glasses is the only kind of glass could be shattered with 60W acoustic wave.

REFERENCES

ASHORY, M. R. Assessment of the massloading effects of accelerometers in modal testing. Proceedings of the 20th International Modal Analysis Conference, 2002. 1027-1031.

BEATTIE, A. 1983. Acoustic emission, principles and instrumentation. Sandia National Labs., Albuquerque, NM (USA).

BLOSS, B. & RAO, M. D. 2002. Measurement of damping in structures by the power input method. *Experimental Techniques,* 26**,** 30-32.

BUTTERS, J. & LEENDERTZ, J. 1971. Speckle pattern and holographic techniques in engineering metrology. *Optics & laser technology,* 3**,** 26-30.

CHANG-HUI, Z. 2005. Sound-frequency method for enhancing the measuring precision of natural frequency and its application in engineering [J]. *Journal of Hefei University of Technology (Natural Science),* 12**,** 017.

FEI, H., AO, Z., FANG, L., CHANGQING, S. & FANRANG, K. Measurement of natural frequencies for the components of the train wheel-bearing based on acoustic method. Advanced Computational Intelligence (ICACI), 2012 IEEE Fifth International Conference on, 18-20 Oct. 2012 2012. 1173-1176.

FELDMAN, B. J. 2003. What to say about the Tacoma Narrows Bridge to your introductory physics class. *The Physics Teacher,* 41**,** 92.

HE, X., NG, T., SIVASHANKER, S. & LIEW, K. 2001. Active control of FGM plates with integrated piezoelectric sensors and actuators. *International Journal of Solids and Structures,* 38**,** 1641-1655.

HU, Y., GAO, Y., SINGAMANENI, S., TSUKRUK, V. V. & WANG, Z. L. 2009. Converse piezoelectric effect induced transverse deflection of a free-standing ZnO microbelt. *Nano letters,* 9**,** 2661-2665.

HUANG, C.-H. & MA, C.-C. 1998. Vibration characteristics for piezoelectric cylinders using amplitude-fluctuation electronic speckle pattern interferometry. *AIAA journal,* 36**,** 2262-2268.

HUANG, C.-H., MA, C.-C. & LIN, Y.-C. 2005. Theoretical, numerical, and experimental investigation on resonant vibrations of piezoceramic annular disks. *Ultrasonics, Ferroelectrics and Frequency Control, IEEE Transactions on,* 52**,** 1204-1216.

JURY, B. F. 2000. Stress testing and relieving method and apparatus. Google Patents.

KERBEL, B. & ARTJUHINA, L. Employment piezoelectric transducers in force-meter equipment. Science and Technology, 2000. KORUS 2000. Proceedings. The 4th Korea-Russia International Symposium on, 2000 2000. 84-88 vol. 3.

LIN, H.-Y., HUANG, J. H. & MA, C.-C. 2002. Vibration analysis of piezoelectric materials by optical methods. *Ultrasonics, Ferroelectrics and Frequency Control, IEEE Transactions on,* 49**,** 1139-1149.

LIN, Y.-C. & MA, C.-C. 2004. Experimental measurement and numerical analysis on resonant characteristics of piezoelectric disks with partial electrode designs. *Ultrasonics, Ferroelectrics and Frequency Control, IEEE Transactions on,* 51**,** 937-947.

MA, C.-C. & HUANG, C.-H. 2001. The investigation of three-dimensional vibration for piezoelectric rectangular parallelepipeds using the AF-ESPI method. *Ultrasonics, Ferroelectrics and Frequency Control, IEEE Transactions on,* 48**,** 142-153.

O'NEILL, J., GENIUS, P. & ANDERSON, L. Nikola Tesla: Mechanical Oscillator.

OKUBO, S. 1984. Stress control in solid materials. Google Patents.

PAVIC, A., ARMITAGE, T., REYNOLDS, P. & WRIGHT, J. 2002. Methodology for modal testing of the Millennium Bridge, London. *Proceedings of the Institution of Civil Engineers. Structures and buildings,* 152**,** 111-121.

SELLAR, J. G. 1991. Apparatus for employing destructive resonance. Google Patents.

TANIGUCHI, R., HATTORI, S., SAKAMOTO, T., SHIMADA, T. & MATSUHASHI, K. 2001. Nondestructive testing apparatus. Google Patents.

TILLY, G. P. 2011. Dynamic behaviour and collapses of early suspension bridges. *Proceedings of the ICE-Bridge Engineering,* 164**,** 75-80.

TZOU, H. & PANDITA, S. 1987. A multi‐purpose dynamic and tactile sensor for robot manipulators. *Journal of robotic systems,* 4**,** 719-741.

TZOU, H. & TSENG, C. 1990. Distributed piezoelectric sensor/actuator design for dynamic measurement/control of distributed parameter systems: a piezoelectric finite element approach. *Journal of Sound and Vibration,* 138**,** 17-34.

WANG, W.-C., HWANG, C.-H. & LIN, S.-Y. 1996. Vibration measurement by the time-averaged electronic speckle pattern interferometry methods. *Applied optics,* 35**,** 4502-4509.

APPENDICES

APPENDIX A: Hardware Photos

NI sbRIO-9632XT board

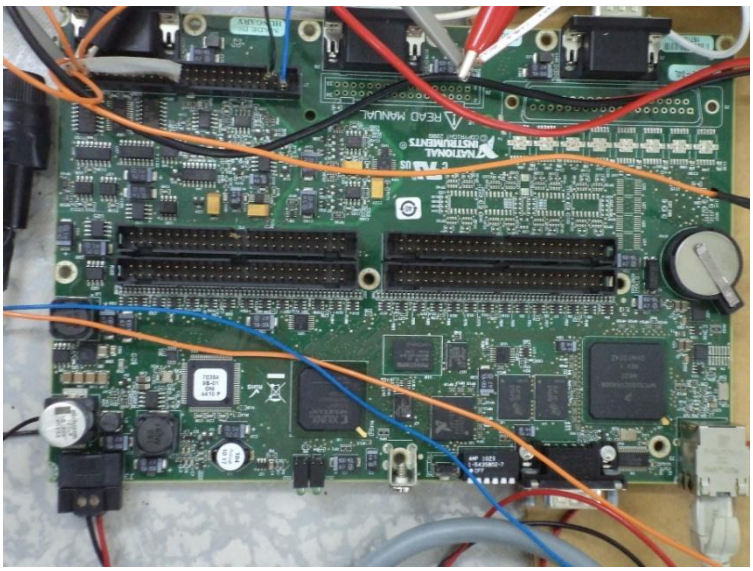

Power Supply for NI sbRIO-9632XT board

Voltage Divider Circuit

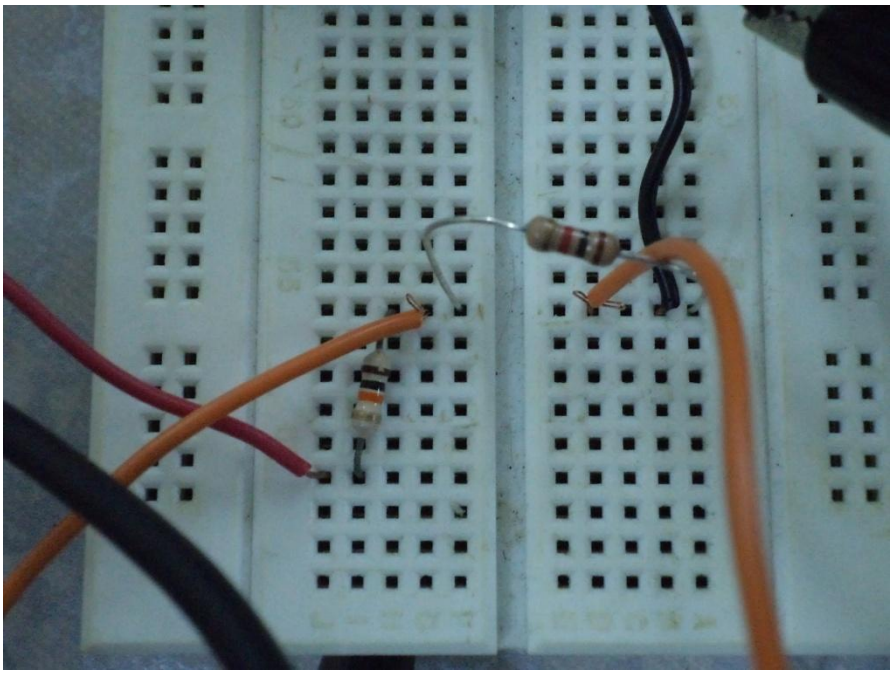

Loudspeaker

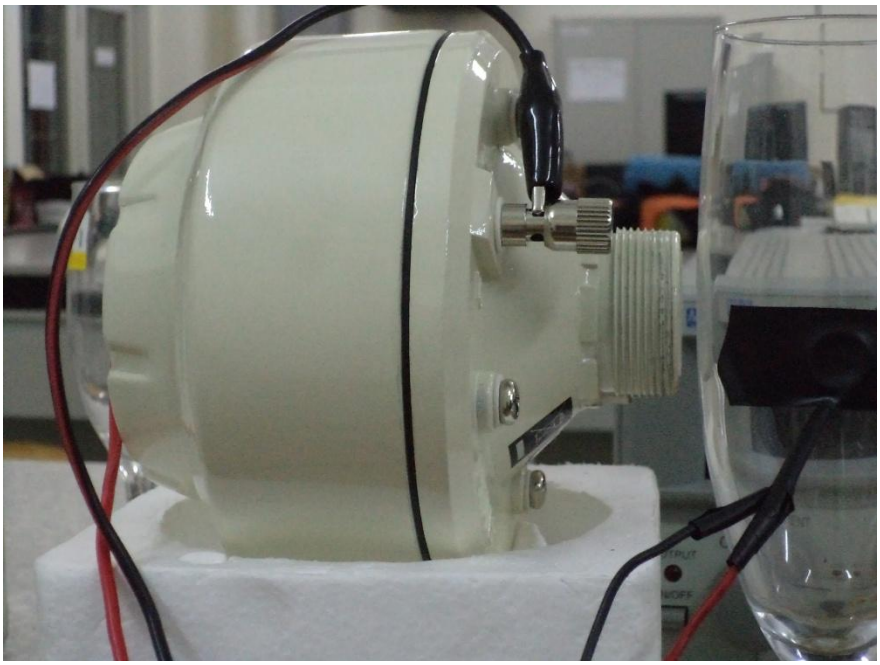

APPENDIX B: LabVIEW codings

List of VIs

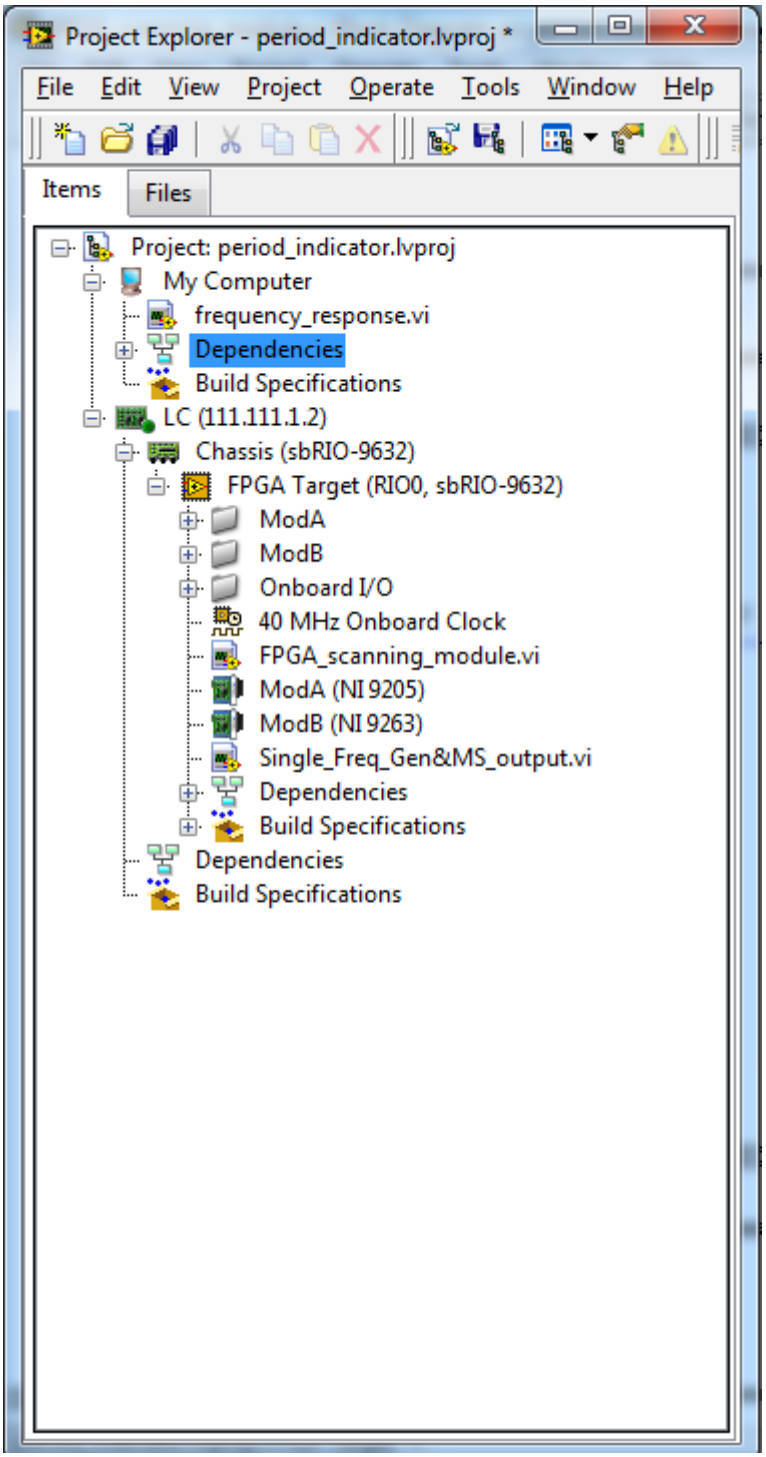

Block Diagram of frequency_response.vi (main program)

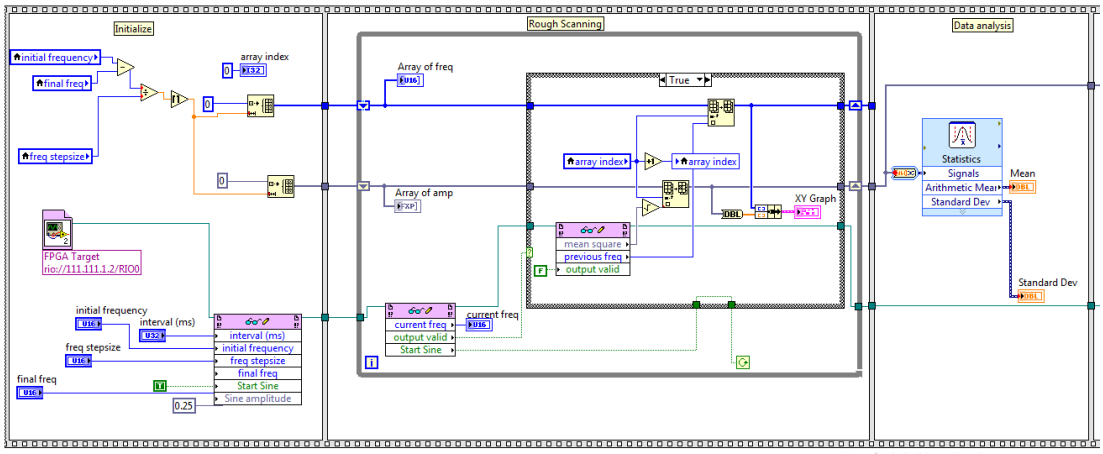

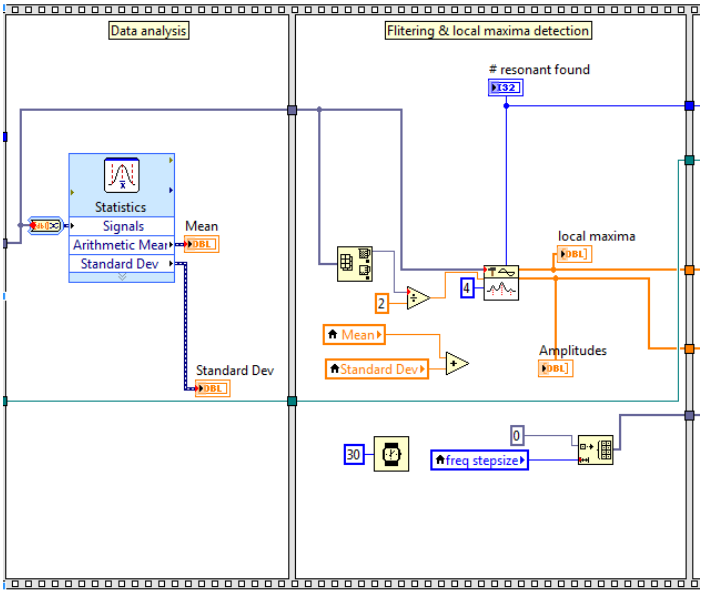

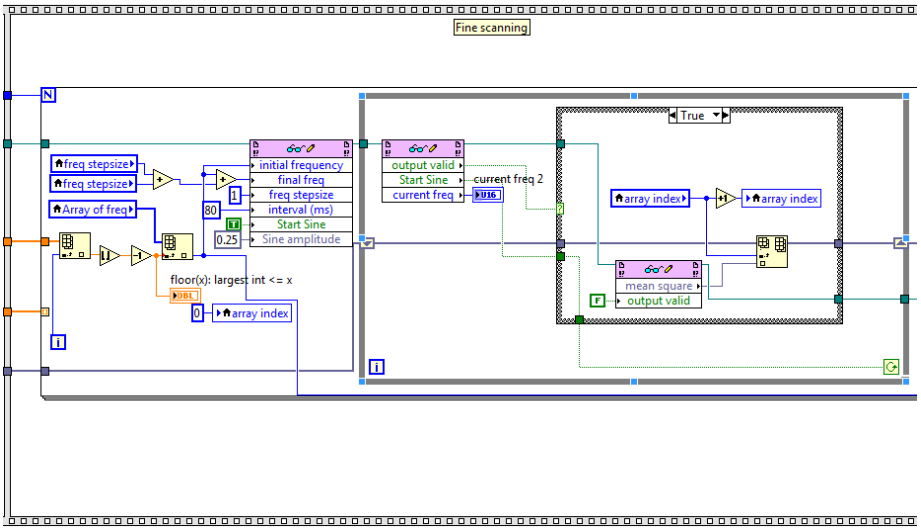

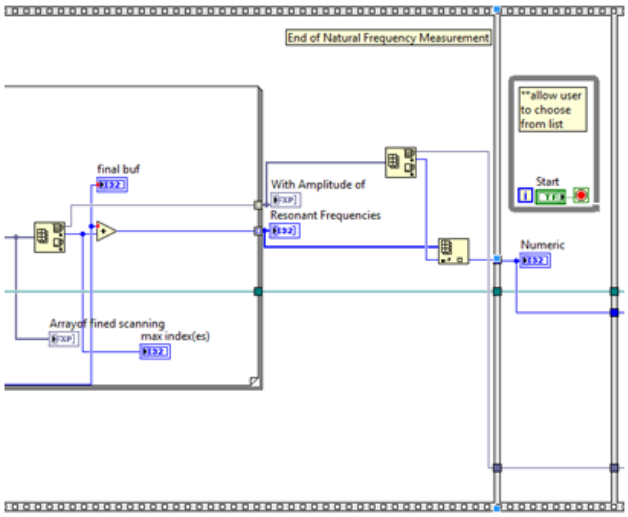
End of Natural Frequency Measurement
**allow user to choose from list
Start
final buf
With Amplitude of
Resonant Frequencies
Numeric
Array of fined scanning max index(es)

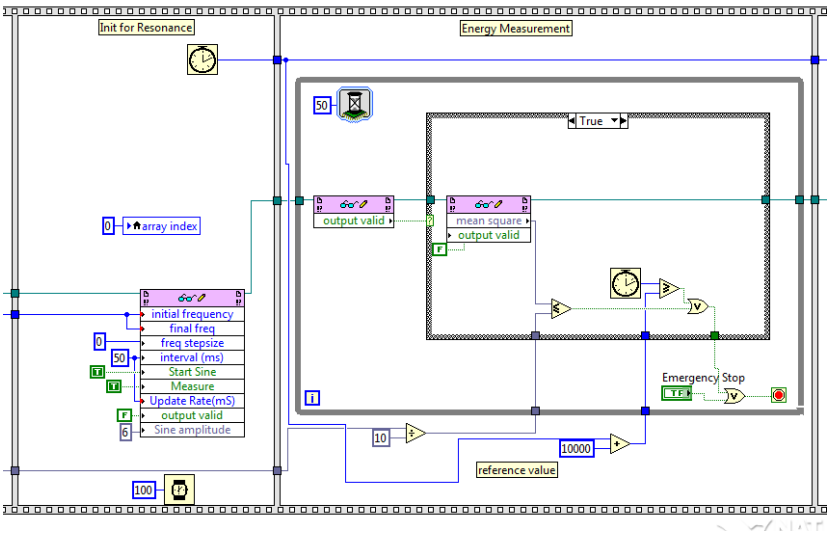
Init for Resonance
Energy Measurement
50
True
output valid
mean square
output valid
0
array index
initial frequency
final freq
freq stepsize
interval (ms)
Start Sine
Measure
Update Rate(mS)
output valid
Sine amplitude
Emergency Stop
10
10000
reference value
100

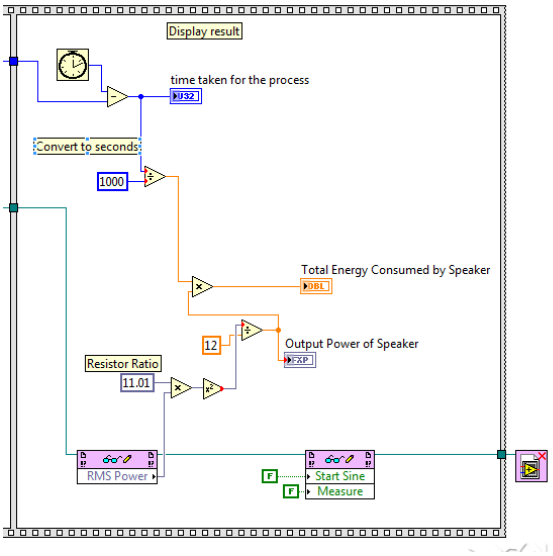
Display result
time taken for the process
Convert to seconds
1000
Total Energy Consumed by Speaker
12
Output Power of Speaker
Resistor Ratio
11.01
RMS Power
Start Sine
Measure

Single_Freq_Gen&MS_output.vi

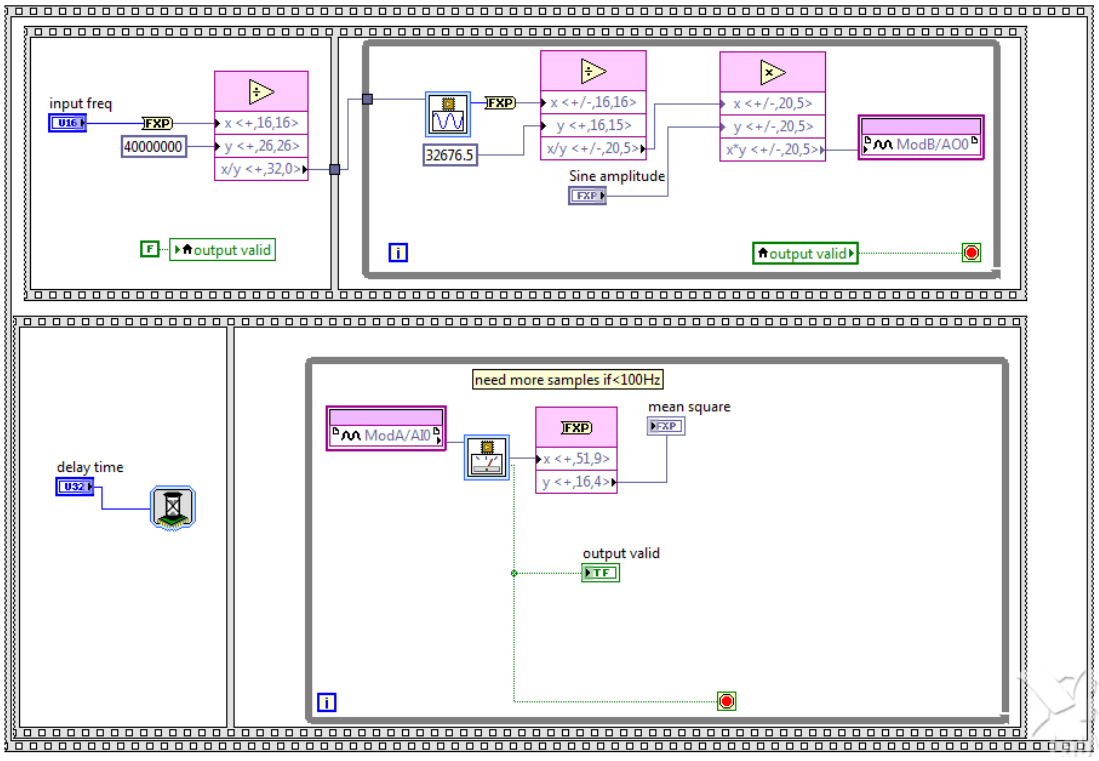

FPGA_scanning_module.VI